

Influence of Alkaline-Peroxide Treatment of Fiber on the Mechanical Properties of Oil Palm Mesocarp Fiber/Poly(butylene succinate) Biocomposite

Yoon Yee Then,^a Nor Azowa Ibrahim,^{a,*} Norhazlin Zainuddin,^a
Buong Woei Chieng,^a Hidayah Ariffin,^b and Wan Md Zin Wan Yunus^c

In this work, the surface of oil palm mesocarp fiber (OPMF) was modified *via* alkaline-peroxide treatment with hydrogen peroxide under alkaline conditions. The effect of the treatment on the chemical composition and microstructure of the fiber was examined using chemical analysis, Fourier transform infrared (FTIR) spectroscopy, scanning electron microscopy (SEM), and X-ray diffraction (XRD) analysis. The treatment resulted in the removal of lignin, hemicellulose, and waxy substances from the fiber and increased its surface roughness and crystallinity. The eco-friendly biocomposite was made from poly(butylene succinate) (PBS) and chemically treated fiber at a weight ratio of 30:70, and was fabricated *via* a melt-blending technique followed by hot-pressed moulding. The results indicated that alkaline-peroxide treatment of the fiber improved the tensile strength, tensile modulus, and elongation at break of the OPMF/PBS biocomposite by 54, 830, and 43%, respectively. The SEM analysis revealed improvement of the interfacial adhesion between the chemically treated fiber and the PBS. This work demonstrates that alkaline-peroxide treatment of fiber is beneficial prior to its use in fabricating biocomposites.

Keywords: Alkaline-peroxide; Biocomposite; Oil palm mesocarp fiber; Poly(butylene succinate)

Contact information: a: Department of Chemistry, Faculty of Science, Universiti Putra Malaysia, 43400 UPM Serdang, Selangor, Malaysia; b: Department of Bioprocess Technology, Faculty of Biotechnology and Biomolecular Sciences, Universiti Putra Malaysia, 43400 UPM Serdang, Selangor, Malaysia; c: Department of Chemistry, Centre For Defence Foundation Studies, National Defence University of Malaysia, Sungai Besi Camp, 57000 Kuala Lumpur, Federal Territory of Kuala Lumpur, Malaysia; * Corresponding author: norazowa@upm.edu.my

INTRODUCTION

The majority of plastic products used today are derived from nonrenewable petrochemical resources and are not biodegradable. These products contribute to pollution long after their functional life due to littering and waste disposal problems. This has triggered a search for biodegradable plastics, especially those derived from renewable resources, as substitutes for petrochemical-based, non-biodegradable plastics (Song *et al.* 2009). Recently, several types of biodegradable plastics have been introduced into the market. However, due to their relatively high production costs, these types of plastics cannot economically compete with the conventional plastics already present in the market. Researchers have combined these biodegradable plastics with inexpensive fillers, particularly lignocellulosic materials obtained from agricultural wastes, to more cost-effectively produce biocomposites (Teh *et al.* 2013; Abdul Razak *et al.* 2014; Rayung *et al.* 2014). According to recent publications, a wide range of lignocellulosic materials

including fibers from kenaf (Abdul Razak *et al.* 2014), oil palm (Teh *et al.* 2013; Then *et al.* 2013, 2014a, 2014b, 2014c, 2015; Rayung *et al.* 2014), coir (Nam *et al.* 2011), and jute (Liu *et al.* 2009) have been compounded with various types of biodegradable plastics, particularly poly(lactic acid) (PLA) and poly(butylene succinate) (PBS), to fabricate low-cost, biodegradable biocomposites. These biocomposites have mechanical properties comparable to those of conventional plastics.

According to previous reports, both PLA and PBS are derived from renewable resources and are biodegradable (Suryanegara *et al.* 2009; Xu and Guo 2010). However, PBS is preferable for use in this work due to its relatively low price and low processing temperature (roughly 120 °C), at which there would be little degradation of fiber during the compounding process (Nam *et al.* 2011). The agricultural waste of interest to this study is oil palm mesocarp fiber (OPMF). It can be obtained in large quantities at almost no cost from palm oil mills after oil palm fruit is screw-pressed to produce crude palm oil (Sreekala *et al.* 1997). Additionally, no extra processing aid is required in order to obtain the fiber. These features can be counted as advantages of OPMF as an alternative lignocellulosic material relative to those of commonly used natural fibers such as kenaf and jute, which are purposely cultivated for the production of fiber. Also, additional processing aids are typically needed after harvesting for extracting and separating the fibers from plants. Momentarily, very little research has been conducted on OPMF, especially with respect to the fabrication of biocomposites.

Although biocomposites made from PBS and OPMF are fully biodegradable and price-competitive, this combination has several limitations, including poor interfacial adhesion between the two phases due to their dissimilar surface polarities (Kalia *et al.* 2009). This often leads to biocomposites with relatively poor mechanical properties. Additionally, typical melt-blending of untreated natural fiber with polymer matrices produces biocomposite sheets that are dark brown in color. This has limited its application, especially in products requiring a wide range of colors (Rayung *et al.* 2014). Considerable effort has been made to enhance the mechanical properties and physical appearances of the biocomposites.

In a previous work, OPMF was treated with a number of different modification processes, including chemical grafting (Teh *et al.* 2013), alkalization (Then *et al.* 2015), superheated steam treatment (Then *et al.* 2014a), and a combination of superheated steam and alkali treatments (Then *et al.* 2014c), aiming to improve fiber adhesion to polymer matrices. The modification processes did improve the interfacial adhesion and the mechanical properties of the biocomposites, but the biocomposite sheets remained dark brown in color.

An alkaline-peroxide treatment, normally known as bleaching, is introduced in this work. In this modification process, hydrogen peroxide is used instead of sodium chlorite, a more conventional bleaching agent, making the treatment a chlorine-free process. Under alkaline conditions, hydrogen peroxide can simultaneously decolorize fibers and eliminate surface impurities, hemicellulose, and lignin (Abdul Razak *et al.* 2014). To date, there have been few studies of the use of bleached fiber in biocomposites. Thus, it is worthwhile to investigate the ability of bleaching to improve the mechanical properties and physical appearance of the biocomposites.

The primary goal of this work was to enhance the mechanical properties and physical appearance of OPMF/PBS biocomposite *via* alkaline-peroxide treatment of the fiber. The structural and chemical changes to the fiber that occurred following alkaline-peroxide treatment were characterized by Fourier transform infrared spectroscopy,

scanning electron microscopy, chemical analysis, and X-ray diffraction analysis. The influence of alkaline-peroxide-treated fiber on the tensile, flexural, and impact properties of OPMF/PBS biocomposite were also determined.

EXPERIMENTAL

Materials

Poly(butylene succinate) (PBS), under the trade name of BIONOLLE™ 1903MD, was purchased from Showa Denko (Japan). It has a density of 1.26 g/cm³ and a melting point of approximately 115 °C. Oil palm mesocarp fiber (OPMF) was obtained from FELDA Seriting Hilir Palm Oil Mill (Malaysia). It was washed by soaking in distilled water for 24 h, rinsing with hot water (60 °C), and finally, rinsing with acetone prior to drying in an oven at 60 °C. The fiber was washed to remove dirt from its surface. The dried fiber was then ground, sieved to a particle size of 150 to 300 μm, and stored in a sealed polyethylene bag for later use in the chemical treatment process and biocomposite fabrication. The properties of OPMF can be found in a previous report (Then *et al.* 2014d). Sodium chlorite (NaClO₂) was purchased from Acros Organics (Belgium). The NaOH pellets, KOH pellets, and H₂SO₄ were purchased from Merck (Germany). Hydrogen peroxide (30%) was supplied by J. T. Baker (USA). All chemicals were of analytical grade and used as received.

Methods

Modification of OPMF by alkaline-peroxide treatment

The OPMF was oven-dried at 60 °C prior to the modification process. The untreated OPMF was subjected to an alkaline-peroxide treatment with 7% hydrogen peroxide at pH 11 and 70 °C for 90 min. The pH of the solution was adjusted using 1 M NaOH solution. The weight ratio of fiber-to-solution was fixed at 1:20. After the treatment, the fiber was filtered, washed several times with water until a neutral pH was achieved, and dried in an oven at 60 °C for 24 h. The alkaline-peroxide treated OPMF was labeled as BOPMF.

Preparation of biocomposites

The PBS and fibers (OPMF or BOPMF) were oven-dried at 60 °C prior to use. The biocomposites were prepared by melt-blending PBS and fibers at a weight ratio of 30:70 in a Brabender internal mixer (Germany) at 120 °C with 50 rpm rotor speed for 15 min, as reported by Then *et al.* (2013). To summarize, the PBS pellet was loaded into the mixer chamber for 2 min to melt. Next, fibers were slowly added into the mixing chamber and mixing continued for another 13 min. These compounded materials were then compressed to 1- and 3-mm thick sheets with lengths of 150 mm and widths of 150 mm. A hydraulic hot-press at 120 °C was used to press the compounded materials for 5 min under 150 kgf/cm² pressure, followed by cold pressing at 30 °C for 5 min.

Fourier Transform Infrared Spectroscopy (FTIR)

The functional groups, types of bonds, and chemical components of the fibers were identified using a Perkin Elmer Spectrum 100 series Spectrophotometer (USA) equipped with attenuated total reflectance (ATR) capability. The FTIR spectra of the

fibers were recorded in the frequency range of 400 to 4000 cm^{-1} with 16 scans in each case at a resolution of 4 cm^{-1} .

Chemical analysis

The chemical component (*i.e.*, cellulose, hemicellulose, and lignin) contents of the fibers were determined using chemical analysis according to the standard procedures described by Abe *et al.* (2007). The holocellulose (cellulose and hemicellulose) content of fibers was determined by gradually removing the lignin by treating the fibers with 5 wt.% NaClO_2 solution at 70 °C for 1 h at a fiber-to-liquor weight ratio of 1:20. The pH of the solution was adjusted to 4 with H_2SO_4 solution. The solid residue was filtered, washed, and then oven-dried at 60 °C until a constant weight was achieved. The cellulose content was determined by treating the holocellulose with 6 wt.% potassium hydroxide solution for 24 h at 25 °C. The solid residue was then filtered, washed, and oven-dried at 60 °C until a constant weight was achieved.

The hemicellulose content was determined as the difference between the holocellulose and cellulose contents of the fibers. To determine the lignin content, the fibers were immersed in 72% H_2SO_4 solution at 30 °C for 1 h, after which the solution was diluted to 3% acid concentration and maintained in reflux for 2 h. The insoluble residue was filtered, washed, and oven-dried at 60 °C until a constant weight was obtained.

To determine the moisture content, weighed quantities of OPMF and BOPMF were placed in an oven at 105 °C for 4 h. The weight of the oven-dried fibers was measured. The difference in weight corresponded to the moisture content of the fibers. The ash content was determined by heating the fibers in the furnace at 550 °C for 2 h. The fibers were then cooled in a desiccator and weighed to determine their ash content. The average values of three replicate samples were recorded.

X-Ray Diffraction (XRD) analysis

The crystallinity of the OPMF and BOPMF was determined using a Shimadzu XRD 6000 Diffractometer (Japan) with a nickel-filtered $\text{Cu K}\alpha$ ($\lambda = 0.1542$ nm) beam operated at 30 kV and 30 mA. The fibers were scanned within a 2θ range of 10 to 30° with scanning rate of 2°/min at 25 °C. The crystallinity index (*CrI*) was calculated from the XRD data and determined based on Eq. (1), as stated by Segal *et al.* (1959):

$$CrI (\%) = \frac{I_{002} - I_{am}}{I_{002}} \times 100 \quad (1)$$

where I_{002} was the maximum intensity of diffraction of the (002) lattice peak at a 2θ of 22 to 23° and I_{am} is the intensity of diffraction of the amorphous material, which was taken at a 2θ of 18°, where the intensity is at a minimum.

Scanning Electron Microscopy (SEM)

The microstructures of OPMF and BOPMF, as well as the tensile fracture surfaces of the biocomposites, were studied using a JEOL JSM-6400 scanning electron microscope (Japan) operated at a 15 kV accelerating voltage. The oven-dried fibers were placed on the metal holder and coated with gold with a Bio-Rad sputter coater (USA) for 3 min to ensure good conductivity prior to analysis.

Mechanical properties measurements

A tensile test was carried out on the biocomposites using a Universal Testing Machine-Instron 4302 (USA) equipped with 1-kN load cell. The test specimens were cut from 1-mm sample sheets using a dumbbell shaped cutter as specified by ASTM D638-5 (2000). A crosshead speed of 5 mm/min was used and the tests were performed at 25 °C. The tensile strength, tensile modulus, and elongation at break were reported.

A three-point bending flexural test was conducted using a Universal Testing Machine-Instron 4302 (USA) equipped with 1-kN load cell on the biocomposites according to ASTM D790 (2000). Rectangular test specimens with dimensions of 127.0 mm × 12.7 mm × 3.0 mm (length × width × thickness) were cut from the sample sheets for testing. The test was conducted at 25 °C with a crosshead speed of 1.3 mm/min and a span length of 48 mm. The results were expressed in terms of flexural strength and flexural modulus.

An un-notched Izod impact test was carried out on the biocomposites using an IZOD impact tester (India) equipped with a 7.5-J pendulum at 25 °C according to ASTM D256 (2000). The test specimens were cut to dimensions of 64.0 mm × 12.7 mm × 3.0 mm (length × width × thickness), and impact strength was reported.

The above tests were performed on five specimens for each formulation and the average values and standard deviations were reported.

RESULTS AND DISCUSSION

In this work, alkaline-peroxide treatment with 7% hydrogen peroxide at pH 11 and 70 °C for 90 min was used because these conditions yielded the optimum tensile properties of the biocomposites as determined during preliminary tests.

Characterizations of Fibers

Physical appearances

As shown Fig. 1, alkaline-peroxide treatment with hydrogen peroxide (H₂O₂) had a pronounced effect on the brightness of the fiber.

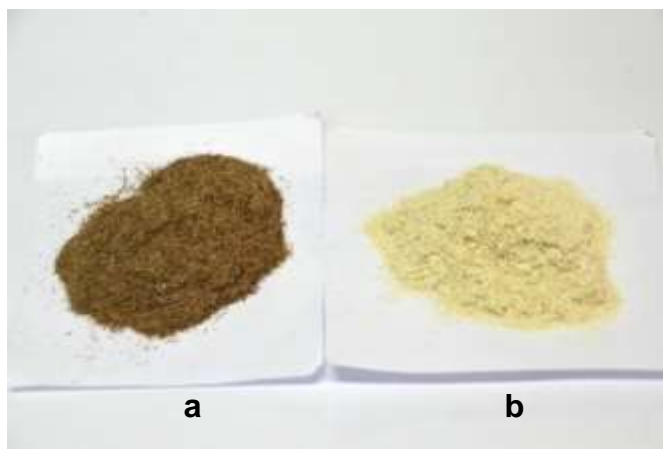
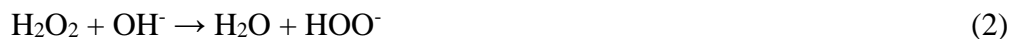


Fig. 1. Photographs (a) OPMF and (b) BOPMF

The initial brown colour of OPMF transitioned into a light yellow colour (BOPMF) after bleaching, indicating that using H₂O₂ as an oxidizing bleaching agent can brighten the fiber. According to Maekawa *et al.* (2007), H₂O₂ easily dissociates into perhydroxyl ions (HOO⁻) under alkaline conditions, as shown in Eq. (2):



These ions are responsible for the decolourization of the fiber *via* attack of the light-absorbing chromophoric groups of lignin and cellulose (carbonyl groups, conjugated carbonyl groups, and quinones) (Sundara 1998).

Fourier transform infrared spectroscopy (FTIR)

Fourier transform infrared spectroscopy (FTIR) was used to study the effects of alkaline-peroxide treatment on the functional groups, types of bonds, and chemical compositions of the fibers. The FTIR spectra of OPMF and BOPMF are shown in Fig. 2.

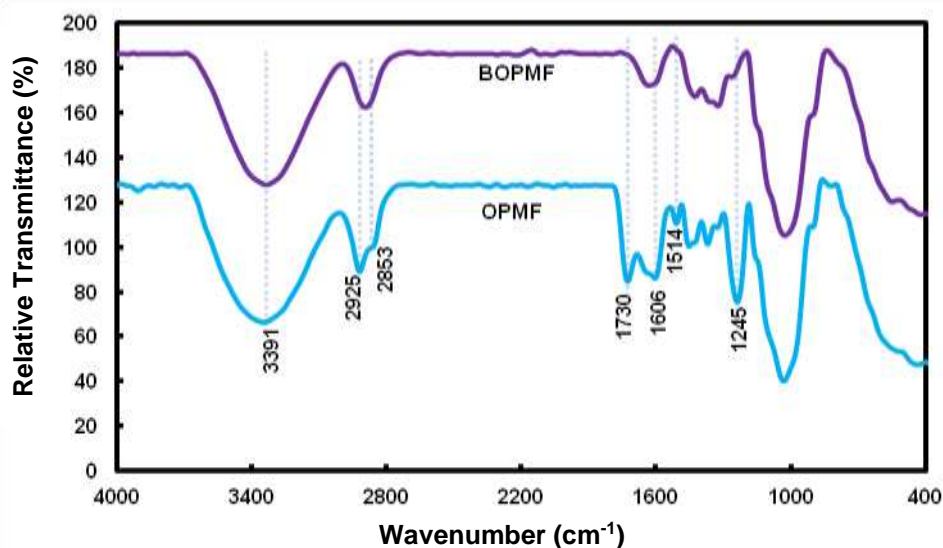


Fig. 2. FTIR spectra of OPMF and BOPMF

Both spectra exhibited broad hydroxyl peaks at 3391 cm⁻¹ corresponding to the O-H stretching of cellulose and hemicellulose. The absorption peaks at 2925 and 2853 cm⁻¹ were attributed to the C-H stretching of cellulose and hemicellulose (Wang *et al.* 2009). A peak at 1730 cm⁻¹ was noted in the spectrum of OPMF but was absent from the BOPMF spectrum. This peak is related to the C=O stretching of carbonyl groups in hemicellulose or lignin (Sreekala *et al.* 2000). The disappearance of this peak can be explained by the elimination of hemicellulose and lignin from the fiber during the alkaline-peroxide treatment. Similar observations have also been reported by other researchers (Rayung *et al.* 2014; Abdul Razak *et al.* 2014; Then *et al.* 2014d). In addition, the intensity of the peaks at 1606 and 1514 cm⁻¹, corresponding to the C=C stretching of aromatic rings in lignin, was relatively low in the spectrum of BOPMF compared to that of OPMF (Xiao *et al.* 2001). A reduction in peak intensity was also noted for the peak at 1245 cm⁻¹, corresponding to the C-O vibration of esters, ethers, and phenol groups in waxy substances or the C-O stretching of the acetyl groups in hemicellulose (Herrera-

Franco and Valadez-Gonzalez 2005; Sinha and Rout 2009). The decreases in the intensity of the peaks at 1606, 1514, and 1245 cm^{-1} in the spectrum of BOPMF demonstrated the partial elimination of hemicellulose, lignin, and waxy substances during the treatment process. These results were further confirmed by the chemical analysis of the fibers.

Chemical analysis

The results of the chemical analysis of OPMF and BOPMF are shown in Table 1. The OPMF contained 32.22% cellulose, whereas BOPMF contained 65.92% cellulose, representing a 105% increase. Meanwhile, decreases in the hemicellulose and lignin content were noted for BOPMF relative to OPMF. This indicates that alkaline-peroxide treatment selectively eliminated lignin and hemicellulose, subsequently increasing the percentage of cellulose in the BOPMF. This result is in agreement with the FTIR results. It is known that lignin is more hydrophobic than hemicellulose or cellulose and that hemicellulose is the most hydrophilic of the three components in fiber and is primarily responsible for moisture absorption. Therefore, the decrease in lignin content makes the fiber more susceptible to moisture absorption. This was clearly shown by the relatively high moisture content of BOPMF compared to that of OPMF. Additionally, the increase in cellulose content and decrease in lignin content in the BOPMF also contributed to a relatively low ash content compared to that of OPMF. Most of the cellulose and hemicellulose are decomposed at 550 °C, as the decomposition temperatures for these two components are between 160 and 400 °C (Yang *et al.* 2007).

Table 1. Chemical Compositions of Fibers

Fibers	Cellulose (%)	Hemicellulose (%)	Lignin (%)	Moisture (%)	Ash (%)
OPMF	32.22 ± 1.54	31.62 ± 0.46	23.89 ± 1.12	7.87 ± 0.70	4.40 ± 0.60
BOPMF	65.92 ± 0.45	13.81 ± 1.23	9.14 ± 0.46	8.84 ± 0.14	2.29 ± 0.25

X-ray diffraction (XRD) analysis

XRD analysis was used to study the structural characteristics and crystallinity of the fibers before and after the treatment process. Figure 3 shows the XRD diffractograms for OPMF and BOPMF.

As shown in Fig. 3, both OPMF and BOPMF exhibited similar XRD patterns with two diffraction peaks at 2θ values of 16.5 (101) and 22.1° (002), corresponding to the crystalline region of fiber. These are typical diffraction patterns for cellulose I (John and Thomas 2008). The non-crystalline region of the fiber is shown by the valley between these two peaks at a 2θ value of 18°, normally denoted I_{am} (Segal *et al.* 1959). It is apparent that the diffraction pattern of BOPMF was very similar to that of OPMF, indicating that alkaline-peroxide treatment did not change the cellulose's crystal structure. This is consistent with the results reported by Joonobi *et al.* (2010) in their work on bleached kenaf core fiber.

As shown in Table 2, the intensities of the peaks at 2θ values of 18 (I_{am}) and 22.1° (I_{002}) changed following alkaline-peroxide treatment, suggesting that the treatment process had an effect on the crystallinity of fiber. The crystallinity indices (CrI) of OPMF and BOPMF, calculated according to Eq. (1), were found to be 33.0 and 65.4%, respectively. The CrI of BOPMF was relatively higher than that of OPMF. Similar observations have also been reported by other researchers (Rayung *et al.* 2014; Abdul Razak *et al.* 2014).

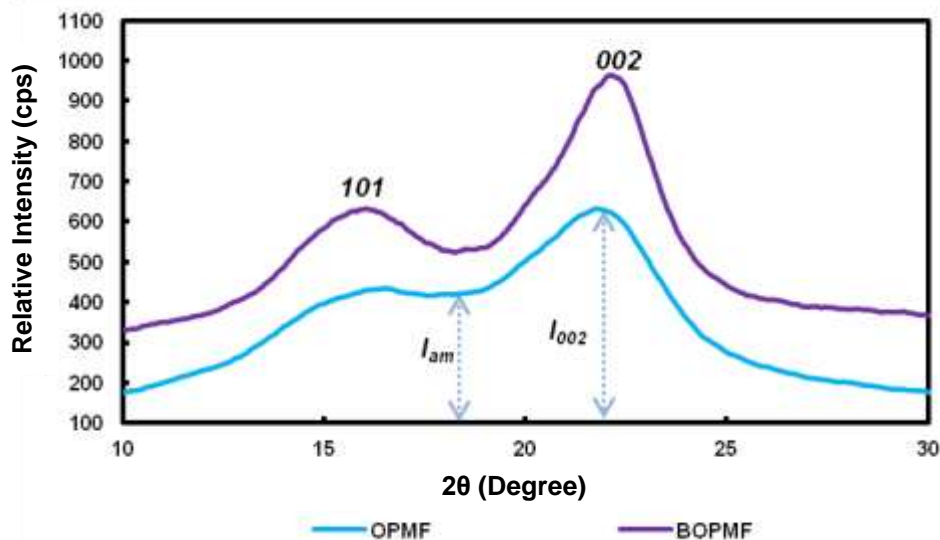


Fig. 3. XRD diffractograms for OPMF and BOPMF

Table 2. Crystallinity Index of Fibers

Fibers	I_{am} (cps)	I_{002} (cps)	CrI (%)
OPMF	348	519	33.0
BOPMF	268	774	65.4

The increase in *CrI* can be attributed to the partial removal of cementing amorphous components, which consist mainly of impurities, hemicellulose, and lignin substances present as consequences of the alkaline-peroxide treatment (Joonobi *et al.* 2010). This result is in agreement with the chemical analysis and FTIR results.

Scanning electron microscopy (SEM)

Scanning electron microscopy (SEM) was used to examine the surface morphology of the fiber following the alkaline-peroxide treatment process. The SEM micrographs of OPMF and BOPMF with low (left) and high (right) magnifications are shown in Fig. 4.

In nature, OPMF is present in the form of fiber bundles, and each bundle is made up of many microfibrils bound together by hemicellulose and lignin. As shown in Figs. 4a and 4b, the external surface of the OPMF bundle seems to be wrapped by a layer of non-cellulosic substances and impurities. Significant differences in the fiber surface morphologies were noted following alkaline-peroxide treatment. The surface of BOPMF appear relatively clean and porous compared to that of the OPMF. This is because of the partial elimination of hemicellulose, lignin, and waxy substances from the fiber surface. Similar results have also been reported by other researchers (Rayung *et al.* 2014; Abdul Razak *et al.* 2014). Additionally, the partial removal of those substances during the treatment process gradually revealed silica particles that were previously embedded in the fiber bundle during the growth of the cell wall. It is notable that some of these silica particles detached, leaving microvoids on the surface of the OPMF. Upon closer examination, microfibrils are seen on the surfaces of BOPMF, but not on OPMF. This may be attributed to the great reduction in the hemicellulose and lignin contents of the

BOPMF, as determined by chemical analysis. This can contribute to the partial separation of fiber bundles, leading to the exposure of microfibrils previously bound together by hemicellulose and lignin. A similar observation was also reported by Joonobi *et al.* (2010) in work with bleached kenaf core fiber.

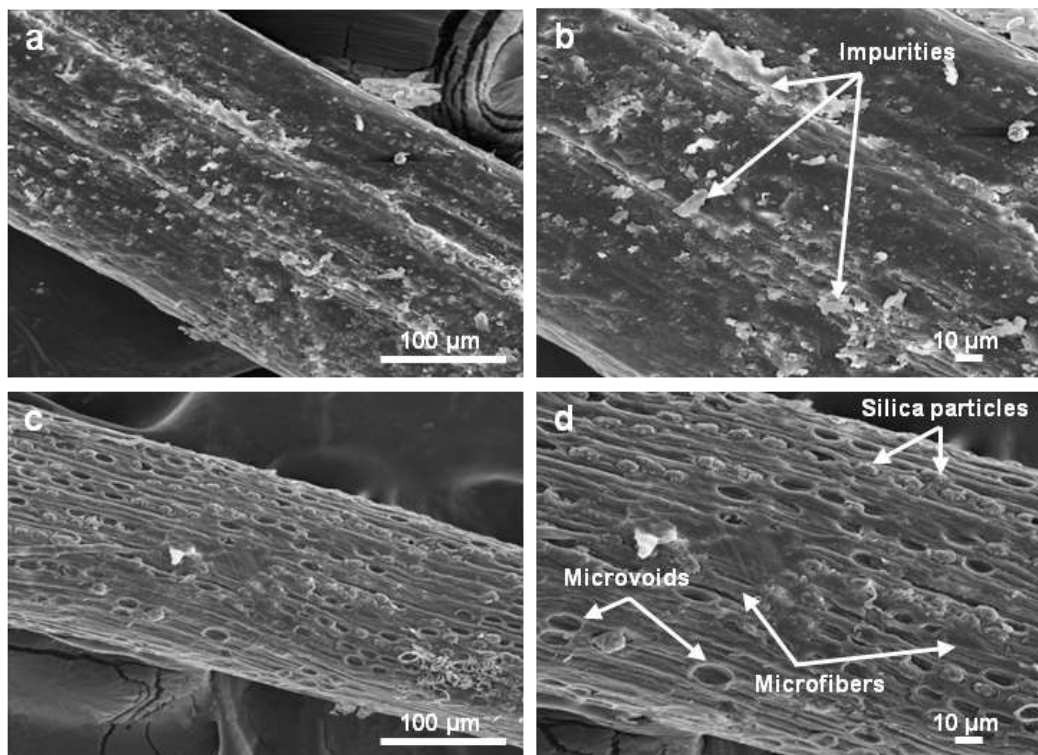


Fig. 4. SEM micrographs of (a and b) OPMF and (c and d) BOPMF

Characterizations of Biocomposites

Physical appearances

A photograph of unmodified PBS, OPMF/PBS, BOPMF/PBS, and BOPMF/PBS/masterbatch biocomposites is shown in Fig. 5. Unmodified PBS is a semi-crystalline polymer, and the product sheet is white in colour. It was noticed that after melt-blending PBS with OPMF, the product became dark brown. This colour is that of the fiber itself, as OPMF is naturally brown. Conversely, the melt-blending of PBS and BOPMF yielded a product sheet with a relatively bright colour as compared to that of the OPMF/PBS sheet. The removal of lignin during the alkaline-peroxide treatment contributed to this colour change.

To produce product sheets with a wide range of colour, a plastic colorant normally known as masterbatch was added to the BOPMF/PBS biocomposite. It is interesting to note that addition of masterbatch in quantities as low as 0.5 wt.% can produce product sheets with different colours (green and red). On the other hand, adding masterbatch to the OPMF/PBS did not yield sheets of different colours, probably due to their initial dark brown colour. This result indicated that alkaline-peroxide treatment of fiber was a beneficial treatment process for producing product sheets with better appearances following the introduction of plastic colorant.

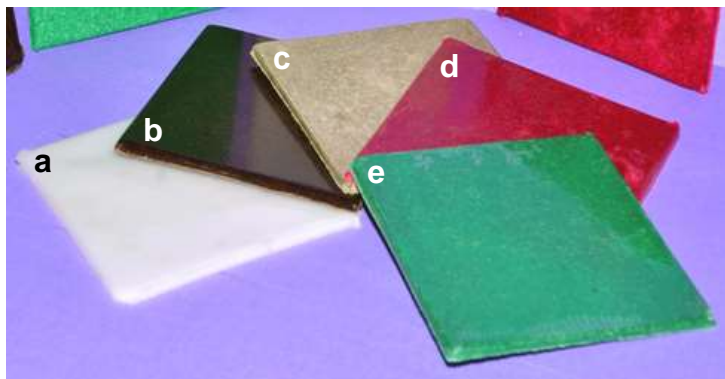


Fig. 5. Photographs of (a) PBS, (b) OPMF/PBS, (c) BOPMF/PBS, and (d, e) BOPMF/PBS/Masterbatch biocomposites

Mechanical properties

In this work, the mechanical properties of the biocomposites were characterized using tensile, flexural, and impact tests. The mechanical properties of the biocomposites are directly proportional to the adhesion strength at the interface of the fibers and the thermoplastic. Generally, stronger adhesion strength results in biocomposites with greater mechanical properties.

The tensile, flexural, and impact strengths of OPMF/PBS and BOPMF/PBS biocomposites are plotted in Fig. 6. As reported in a previous work (Then *et al.* 2013), the tensile strength (TS), flexural strength (FS), and impact strength (IS) of unmodified PBS were 37.31 MPa, 37.58 MPa, and 416.96 J/m, respectively.

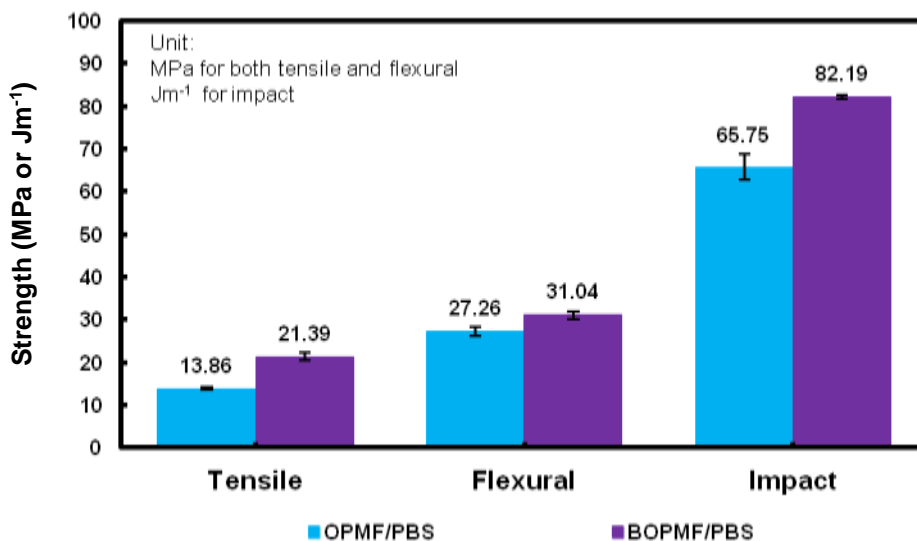


Fig. 6. Tensile, flexural, and impact strengths of OPMF/PBS and BOPMF/PBS biocomposites. Data presented as the mean \pm standard deviation.

As shown in Fig. 6, the introduction of 70 wt.% OPMF to PBS (OPMF/PBS) drastically decreased the TS, FS, and IS to 13.86 MPa, 27.26 MPa, and 65.75 J/m, respectively. This could be due to inefficient stress transfer across the PBS-OPMF interface when load was applied to the biocomposite, resulting from weak interfacial adhesion between the two phases. Additionally, the presence of waxy substances

(previously shown in Figs. 4a and 4b) on the surface of OPMF can also restrict the adhesion of fibers within the polymer matrix, further reducing stress transfer efficiency. Fibers also tend to agglomerate, especially at high loading, due to the increase in fiber-fiber interaction, which can result in regions of stress concentration and decrease the energy required for breakage or crack propagation (Karmarkar *et al.* 2007).

It is interesting to note that BOPMF/PBS biocomposites had considerably improved TS, FS, and IS compared to those of OPMF/PBS biocomposites. The increases in TS, FS, and IS of BOPMF/PBS were 54, 14, and 25%, respectively, relative to those of the OPMF/PBS biocomposite. The alkaline-peroxide treatment rendered the fiber surface relatively clean and porous (Figs. 4c and 4d), providing better adhesion and increasing the number of sites available for mechanical interlocking with PBS, ultimately resulting in stronger interfacial bonding within the biocomposite. Furthermore, the removal of hemicellulose and lignin and the increase in cellulose content and crystallinity of the BOPMF also boosted the effectiveness of the fiber as reinforcement within the biocomposite (Bachtiar *et al.* 2008). These results are consistent with those of a previously published study of a bleached kenaf fiber-reinforced PLA biocomposite (Abdul Razak *et al.* 2014).

Figure 7 illustrates the tensile and flexural moduli of OPMF/PBS and BOPMF/PBS biocomposites. The neat PBS had 248.90 MPa and 562.90 MPa tensile modulus (TM) and flexural modulus (FM), respectively, as reported by Then *et al.* (2013). The TM decreased to 94.80 MPa with the incorporation of 70 wt.% OPMF. In contrast, the FM increased to 2191.00 MPa with the incorporation of 70 wt.% OPMF, an increase of 289%. An opposite trend was observed in TM and FM for the OPMF/PBS biocomposite.

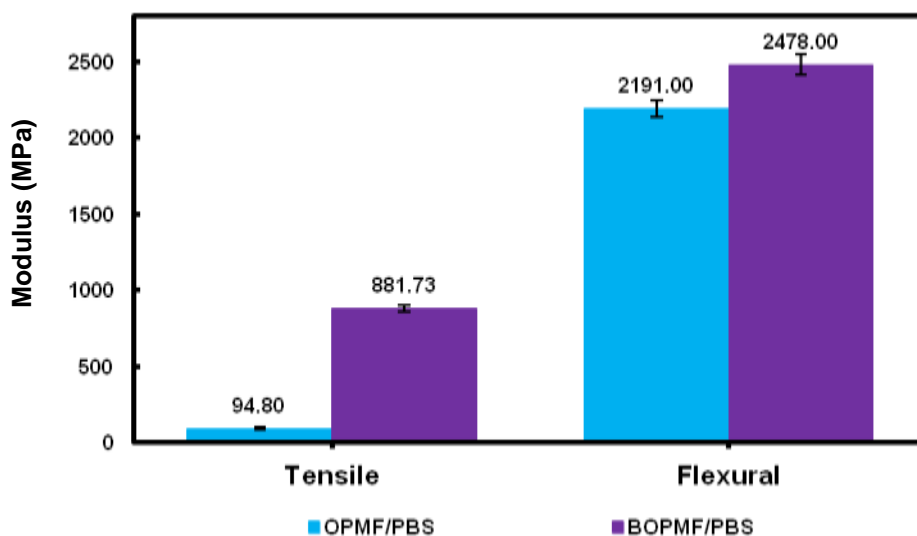


Fig. 7. Tensile and flexural moduli of OPMF/PBS and BOPMF/PBS biocomposites. Data presented as the mean \pm standard deviation.

During the tensile test, all fibers in the biocomposite experienced the same stress, and failure was initiated when the weakest fiber reached its limiting tensile stress. In this work, the fiber content in the biocomposite was relatively high as compared to that in previously published works (Teh *et al.* 2013; Abdul Razak *et al.* 2014; Rayung *et al.* 2014), so the ability of PBS to bind the surrounding OPMF together decreased and the

biocomposite produced was easily deformed and broken under a tensile load. In the flexural test, only a small part of the fibers in the biocomposite were under maximum stress during bending, so the measured FM was higher than the TM for the same material. In addition, the strain rate (5 mm/min and 1.3 mm/min) and thickness of the specimen (1 mm and 3 mm) used for the tensile and flexural tests can also be attributed to the differences in TM and FM. The increase in FM upon the introduction of fiber may be due to the relatively higher stiffness of the fiber compared to that of the polymer matrix. Similar results were also reported by Abdul Razak *et al.* (2014) in a study of a kenaf fiber-PLA biocomposite.

It is interesting to note that, with the substitution of OPMF with BOPMF, the TM and FM of the biocomposites improved considerably. The TM of OPMF/PBS biocomposite was 94.80 MPa and increased dramatically to 881.73 MPa in the BOPMF/PBS biocomposite, an 830% improvement. Since an equal amount of PBS was used in both biocomposites, the improvement in TM was attributed to the increase in the surface wettability of the BOPMF *via* the removal of waxy substances during the alkaline-peroxide treatment process. As a consequence, the ability of PBS to adhere to and subsequently bind the surrounding BOPMF together increased, thereby producing a relatively stiffer biocomposite with a superior TM. The increase in interfacial adhesion between the BOPMF and PBS also enhanced the FM by 13% in the BOPMF/PBS biocomposite.

The elongation at break (EB) of the OPMF/PBS and BOPMF/PBS biocomposites is illustrated in Fig. 8. Neat PBS is a flexible polymer and thereby has a high EB of 470%. Following the incorporation of 70 wt.% OPMF into the PBS matrix, the EB decreased dramatically to 2.50%. The decrease in EB is due to the reduced structural integrity of PBS as well as the rigid, relatively inflexible structure of fiber itself (Liu *et al.* 2009). The EB of the BOPMF/PBS biocomposite increased by 43%, to 3.58%, following the alkaline-peroxide treatment of the fiber. Lignin itself imparts stiffness and rigidity to plants.

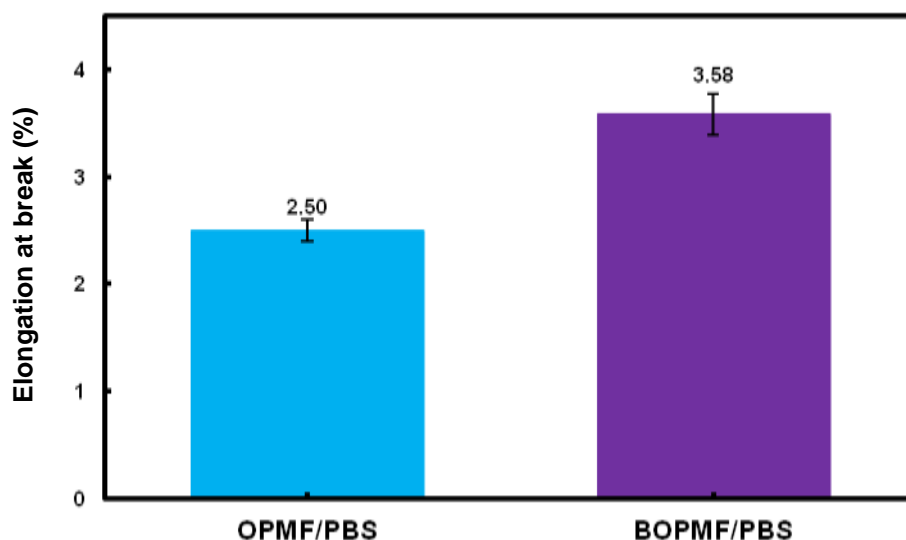


Fig. 8. Elongation at break (EB) of OPMF/PBS and BOPMF/PBS biocomposites. Data presented as the mean \pm standard deviation.

In this work, it was noted that more than 60% of the lignin initially present (Table 1) was eliminated by the alkaline-peroxide treatment process. The elimination of lignin therefore reduced the rigidity of BOPMF and subsequently increased the EB of the BOPMF/PBS biocomposite. This result is in agreement with those reported by Abdul Razak *et al.* (2014) and Rayung *et al.* (2014) in studies of bleached kenaf fiber and oil palm empty fruit bunch fiber reinforced PLA biocomposites.

Interfacial properties

SEM analysis was performed to evaluate the interfacial adhesion between PBS and OPMF or BOPMF. Figure 9 shows the SEM micrographs of the fracture surfaces of the OPMF/PBS and BOPMF/PBS biocomposites after tensile testing. Tensile fracture surface observations are normally used to evaluate the failure mechanism of the particular biocomposite. As can be seen in Figs. 9a and 9b, cavities were present on the fracture surface of the OPMF/PBS biocomposite, likely resulting from fiber pull-out during the tensile test. In addition, a gap at the interface of the PBS and OPMF was also present, attributed either to debonding during the tensile test or to poor contact between the two phases (Bax and Mussig 2008). The presence of cavities and a gap indicate poor interfacial adhesion resulting from the lack of compatibility between hydrophilic fibers and hydrophobic PBS. In general, poor interfacial adhesion causes stress concentration under external loads, resulting in premature failure due to poor stress transfer across the fiber-matrix interface (Yang *et al.* 2006). This explains the decreases in TS, FS, and IS upon introduction of 70 wt.% OPMF to the PBS matrix.

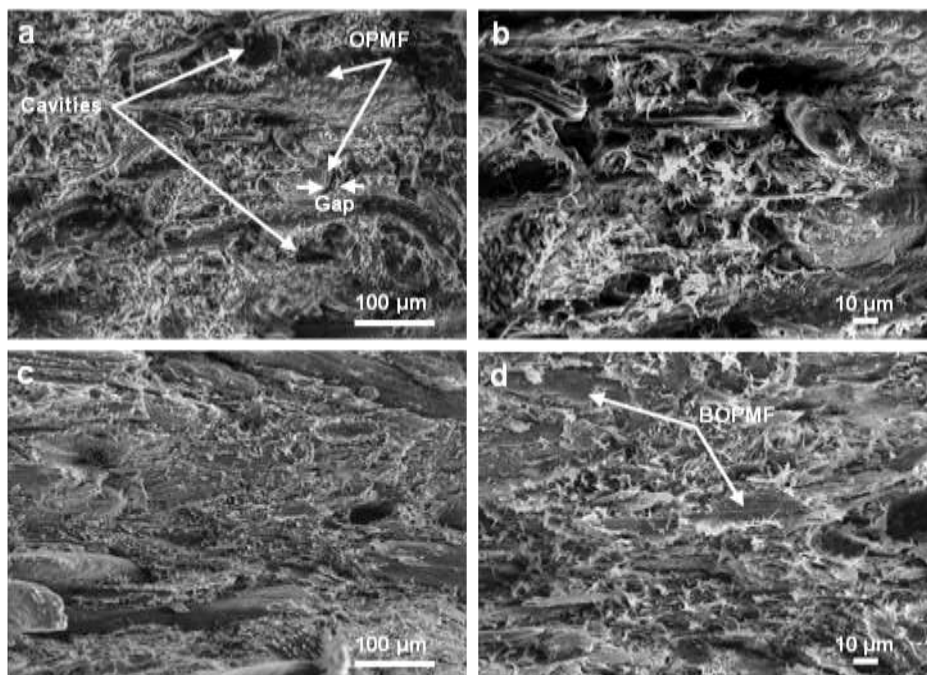


Fig. 9. SEM micrographs of the tensile fracture surfaces of (a and b) OPMF/PBS and (c and d) BOPMF/PBS biocomposites at low (a and c) and high (b and d) magnification

In the presence of BOPMF, fewer cavities resulted from fiber pull-out, as shown in the micrograph of the BOPMF/PBS biocomposite (Figs. 9c and 9d). Additionally, the contact between the BOPMF and PBS was also considerably improved, as indicated by

the absence of a gap at the BOPMF/PBS interface. These observations clearly indicate that the alkaline-peroxide treatment process improved the adhesion characteristics of fiber toward the polymer matrix, most likely due to the removal of surface impurities and the generation of microvoids during the treatment process. The relatively clean surface of the BOPMF and the presence of microvoids were important in promoting adhesion between fiber and the polymer *via* a mechanical interlocking mechanism. These observations also explain why the BOPMF/PBS biocomposite exhibited greater mechanical properties than the OPMF/PBS biocomposite.

CONCLUSIONS

1. The surface of OPMF was successfully modified by alkaline-peroxide treatment, yielding treated fiber with a relatively bright colour.
2. The alkaline-peroxide treatment of fiber eliminated most of the lignin, hemicellulose, and waxy substances from the fiber, subsequently increasing the cellulose fraction and crystallinity index of the treated fiber.
3. The introduction of treated fiber into PBS resulted in a biocomposite with better physical appearance and that can be further modified with plastic colorants.
4. The tensile, flexural, and impact properties of the biocomposite were considerably improved by the presence of treated fiber.
5. This work demonstrated that alkaline-peroxide treatment of fiber is beneficial in producing biocomposites with enhanced mechanical performance along with better physical appearance.

ACKNOWLEDGMENTS

The authors would like to acknowledge the Ministry of Education, Malaysia, for their provision of a scholarship (MyPhD). The authors would also like to thank the Exploratory Research Grant Scheme (ERGS) from the Ministry of Higher Education (MOHE), Malaysia for their financial support.

REFERENCES CITED

- ASTM D256. (2000). "Standard test methods for determining the Izod pendulum impact resistance of plastics," *American Society of Testing and Materials*, West Conshohocken, PA.
- ASTM D638-5. (2000). "Standard test method for tensile properties of plastics," *American Society of Testing and Materials*, West Conshohocken, PA.
- ASTM D790. (2000). "Standard test method for flexural properties of unreinforced and reinforced plastics," *American Society of Testing and Materials*, West Conshohocken, PA.
- Abdul Razak, N. I., Ibrahim, N. A., Zainuddin, N., Rayung, M., and Saad, W. Z. (2014). "The influence of chemical surface modification of kenaf fiber using hydrogen

- peroxide on the mechanical properties of biodegradable kenaf fiber/poly(lactic acid) composites,” *Molecules* 19(3), 2957-2968. DOI: 10.3390/molecules19032957
- Abe, K., Iwamoto, S., and Yano, H. (2007). “Obtaining cellulose nanofibers with a uniform width of 15 nm from wood,” *Biomacromolecules* 8(10), 3276-3278. DOI: 10.1021/bm700624p
- Bachtiar, D., Sapuan, S. M., and Hamdan, M. M. (2008). “The effect of alkaline treatment on tensile properties of sugar palm fiber reinforced epoxy composites,” *Materials & Design* 29(7), 1285-1290. DOI: 10.1016/j.matdes.2007.09.006
- Bax, B., and Mussig, J. (2008). “Impact and tensile properties of PLA/cordenka and PLA/flax composites,” *Composites Science and Technology* 68(7-8), 1601-1607. DOI: 10.1016/j.compscitech.2008.01.004
- Herrera-Franco, P. J., and Valadez-Gonzalez, A. (2005). “A study of the mechanical properties of short natural-fiber reinforced composites,” *Composites Part B: Engineering* 36(8), 597-608. DOI: 10.1016/j.compositesb.2005.04.001
- John, M. J., and Thomas, S. (2008). “Biofibres and biocomposites,” *Carbohydrate Polymers* 71(3), 343-364. DOI: 10.1016/j.carbpol.2007.05.040
- Joonobi, M., Harun, J., Tahir, P., Zaini, L., Saiful, A. S., and Makinejad, M. (2010). “Characteristics of nanofibers extracted from kenaf core,” *BioResources* 5(4), 2556-2566. DOI: 10.15376/biores.5.4.2556-2566
- Kalia, S., Kaith, B. S., and Kaur, I. (2009). “Pretreatments of natural fibers and their application as reinforcing material in polymer composites - A review,” *Polymer Engineering & Science* 49(7), 1253-1272. DOI: 10.1002/pen.21328
- Karmarkar, A., Chauhan, S. S., Modak, J. M., and Chanda, M. (2007). “Mechanical properties of wood-fiber reinforced polypropylene composites: Effect of a novel compatibilizer with isocyanate functional group,” *Composites Part A: Applied Science and Manufacturing* 38(2), 227-233. DOI: 10.1016/j.compositesa.2006.05.005
- Liu, L. F., Yu, J. Y., Cheng, L. D., and Qu, W. W. (2009). “Mechanical properties of poly(butylene succinate) (PBS) biocomposites reinforced with surface modified jute fibre,” *Composites Part A: Applied Science and Manufacturing* 40(5), 669-674. DOI: 10.1016/j.compositesa.2009.03.002
- Maekawa, M., Hashimoto, A., and Tahara, M. (2007). “Effects of pH in hydrogen peroxide bleaching on cotton fabrics pretreated with ferrous sulphate,” *Textile Research Journal* 77(4), 222-226. DOI: 10.1177/0040517507078795
- Nam, T. H., Ogihara, S., and Tung, N. H. (2011). “Effect of alkali treatment on interfacial and mechanical properties of coir fiber reinforced poly(butylene succinate) biodegradable composites,” *Composites Part B: Engineering* 42(6), 1648-1656. DOI: 10.1016/j.compositesb.2011.04.001
- Rayung, M., Ibrahim, N. A., Zainuddin, N., Saad, W. Z., Abdul Razak, N. I., and Chieng, B. W. (2014). “The effect of fiber bleaching treatment on the properties of poly(lactic acid)/oil palm empty fruit bunch fiber composites,” *International Journal of Molecular Sciences* 15(8), 14728-14742. DOI: 10.3390/ijms150814728
- Segal, L., Creely, J. J., Martin Jr, A. E., and Conrad, C. M. (1959). “An empirical method for estimating the degree of crystallinity of native cellulose using X-ray diffractometer,” *Textile Research Journal* 29(10), 786-794. DOI: 10.1177/004051755902901003
- Sinha, E., and Rout, S. K. (2009). “Influence of fibre-surface treatment on structural, thermal and mechanical properties of jute fibre and its composite,” *Bulletin of Materials Science* 32(1), 65-76. DOI: 10.1007/s12034-009-0010-3

- Song, J. H., Murphy, R. J., Narayan, R., and Davies, G. B. H. (2009). "Biodegradable and compostable alternatives to conventional plastics," *Philosophical Transactions of the Royal Society B: Biological Sciences* 364(1526), 2127-2139. DOI: 10.1098/rstb.2008.0289
- Sreekala, M. S., Kumaran, M. G., and Thomas, S. (1997). "Oil palm fibers: Morphology, chemical composition, surface modification, and mechanical properties," *Journal of Applied Polymer Science* 66(5), 821-835. DOI: 10.1002/(SICI)1097-4628(19971031)66:5<821::AID-APP2>3.0.CO;2-X
- Sreekala, M. S., Kumaran, M. G., Joseph, S., and Jacob, M. (2000). "Oil palm fibre reinforced phenol formaldehyde composites: Influence of fibre surface modifications on the mechanical performance," *Applied Composite Materials* 7(5-6), 295-329. DOI: 10.1023/A:1026534006291
- Sundara, R. (1998). "Hot peroxide bleaching," *Canadian Chemical News* 50(1), 15-17.
- Suryanegara, L., Nakagaito, A. N., and Yano, H. (2009). "The effect of crystallization of PLA on the thermal and mechanical properties of microfibrillated cellulose-reinforced PLA composites," *Composites Science and Technology* 69(7-8), 1187-1192. DOI: 10.1016/j.compscitech.2009.02.022
- Teh, C. C., Ibrahim, N. A., and Wan Yunus, W. M. Z. (2013). "Response surface methodology for the optimization and characterization of oil palm mesocarp fiber-graft-poly(butyl acrylate)," *BioResources* 8(4), 5244-5260. DOI: 10.15376/biores.8.4.5244-5260
- Then, Y. Y., Ibrahim, N. A., Zainuddin, N., Ariffin, H., and Wan Yunus, W. M. Z. (2013). "Oil palm mesocarp fiber as new lignocellulosic material for fabrication of polymer/fiber biocomposites," *International Journal of Polymer Science* 2013, 1-7. DOI: 10.1155/2013/797452
- Then, Y. Y., Ibrahim, N. A., Zainuddin, N., Ariffin, H., Wan Yunus, W. M. Z., and Chieng, B. W. (2014a). "The influence of green surface modification of oil palm mesocarp fiber by superheated steam on the mechanical properties and dimensional stability of oil palm mesocarp fiber/poly(butylene succinate) biocomposite," *International Journal of Molecular Sciences* 15(9), 15344-15357. DOI: 10.3390/ijms150915344
- Then, Y. Y., Ibrahim, N. A., Zainuddin, N., Ariffin, H., Wan Yunus, W. M. Z., and Abd Rahman, M. F. (2014b). "Effect of electron beam irradiation on the tensile properties of oil palm mesocarp fibre/poly(butylene succinate) biocomposites," *International Journal of Automotive and Mechanical Engineering* 10(July-December), 2070-2080. DOI: 10.15282/ijame.10.2014.23.0174
- Then, Y. Y., Ibrahim, N. A., Zainuddin, N., Ariffin, H., and Wan Yunus, W. M. Z. (2014c). "Enhancement of tensile strength of oil palm mesocarp fiber/poly(butylene succinate) biocomposite via superheated steam-alkali treatment of oil palm mesocarp fiber," *Scientific Research Journal* 11(2), 1-12.
- Then, Y. Y., Ibrahim, N. A., Zainuddin, N., Ariffin, H., Wan Yunus, W. M. Z., and Chieng, B. W. (2014d). "Surface modifications of oil palm mesocarp fiber by superheated steam, alkali, and superheated steam-alkali for biocomposite applications," *BioResources* 9(4), 7467-7483. DOI: 10.15376/biores.9.4.7467-7483
- Then, Y. Y., Ibrahim, N. A., Zainuddin, N., Ariffin, H., Wan Yunus, W. M. Z., and Chieng, B. W. (2015). "Static mechanical, interfacial, and water absorption behaviors of alkali treated oil palm mesocarp fiber reinforced poly(butylene succinate) biocomposites," *BioResources* 10(1), 123-136. DOI: 10.15376/biores.10.1.123-136

- Wang, K. B., Jiang, J. X., Xu, F., and Sun, R. C. (2009). "Influence of steaming pressure on steam explosion pretreatment of Lespedeza stalks (*Lespedeza cryobotrya*): Part 1. Characteristic of degraded cellulose," *Polymer Degradation and Stability* 94(9), 1379-1388. DOI: 10.1016/j.polymdegradstab.2009.05.019
- Xiao, B., Sun, X. F., and Sun, R. (2001). "Chemical, structural, and thermal characterizations of alkali-soluble lignins and hemicelluloses, and cellulose from maize stems, rye straw, and rice straw," *Polymer Degradation and Stability* 74(2), 307-319. DOI: 10.1016/S0141-3910(01)00163-X
- Xu, J., and Guo, B. H. (2010). "Poly(butylene succinate) and its copolymers: Research, development and industrialization," *Biotechnology Journal* 5(11), 1149-1163. DOI: 10.1002/biot.201000136
- Yang, H. S., Kim, H. J., Park, H. J., Lee, B. J., and Hwang, T. S. (2006). "Water absorption behavior and mechanical properties of lignocellulosic filler-polyolefin bio-composites," *Composite Structures* 72(4), 429-437. DOI: 10.1016/j.compstruct.2005.01.013
- Yang, H., Yan, R., Chen, H., Lee, D. H., and Zheng, C. (2007). "Characteristics of hemicellulose, cellulose and lignin pyrolysis," *Fuel* 86(12-13), 1781-1788. DOI: 10.1016/j.fuel.2006.12.013

Article submitted: December 5, 2014; Peer review completed: January 24, 2015; Revised version received and accepted: January 27, 2015; Published: January, 29, 2015.